

## Temperature-dependent Landau damping of the acoustic plasmon in a bilayer system

D. S. Kainth, D. Richards, H. P. Hughes, M. Y. Simmons, and D. A. Ritchie  
*Cavendish Laboratory, Madingley Road, Cambridge CB3 0HE, United Kingdom*  
 (Received 20 November 1997)

We report temperature effects in the Landau damping of the acoustic plasmon mode in a double-quantum-well system. Its dispersion has been measured using Raman spectroscopy and modeled within the random-phase approximation (RPA). The Landau damping of the acoustic plasmon has also been modeled within the RPA using a 0-K Hubbard correction, with mixed success. This points to the need for further theoretical work on local-field corrections at higher temperatures, but shows the value of the study of the temperature dependence of Landau damping as a probe of many-body effects. [S0163-1829(98)52404-6]

Many-body interactions in low-dimensional electron systems have attracted considerable interest in recent years,<sup>1</sup> but at zero magnetic field relatively few experimental studies have been able to probe these phenomena reliably.<sup>2-4</sup> Electron bilayers are particularly intriguing in this context because the interlayer Coulomb interaction can counterbalance the kinetic energy of the electrons, allowing many-body effects to dominate.

A two-layer electron system such as a semiconductor double-quantum-well structure supports two plasmon modes corresponding to the in-phase (optic plasmon, OP) and out-of-phase (acoustic plasmon, AP) intra-sub-band oscillations of the charge densities in each layer. These modes have been extensively studied theoretically<sup>5,6</sup> and are ideal testbeds for studying many-body effects. For example, the dispersion of the AP mode is strongly affected by correlations,<sup>7</sup> and both the OP and AP enhance substantially Coulomb drag effects in bilayer systems.<sup>8</sup> Compared with the plasmon for a single two-dimensional electron gas (2DEG), the low-lying AP is also expected to be more susceptible to Landau damping<sup>7,8</sup>—the transfer of energy from the plasmon (a coherent mode) to a single-particle excitation (SPE). Acoustic plasmons may also be involved in mechanisms for high-temperature superconductivity, mediating an attractive interaction between electrons in the conducting layers of such materials.<sup>9</sup>

Inelastic light scattering is used here to probe the plasmon dispersions of a double 2DEG structure as a function of the wave vector, in contrast to transport measurements which effectively integrate over all wave vectors.<sup>4</sup> Temperature-induced Landau damping of the AP mode is also reported, and corresponding random-phase approximation (RPA) calculations (including a 0-K Hubbard correction to account for exchange-correlation effects) show that the temperature dependence of Landau damping is a valuable test in modeling many-body phenomena, particularly at high temperatures.

Three molecular-beam-epitaxy- (MBE) grown samples, *A*, *B*, and *C*, were studied. Each consisted of two modulation-doped GaAs quantum wells of width  $L_w = 200 \text{ \AA}$  (*A*),  $150 \text{ \AA}$  (*B*), and  $180 \text{ \AA}$  (*C*) separated by an  $\text{Al}_{0.67}\text{Ga}_{0.33}\text{As}$  barrier of width  $L_b = 600 \text{ \AA}$  (*A*),  $300 \text{ \AA}$  (*B*), and  $125 \text{ \AA}$  (*C*). The effective inter-2DEG separation  $d$  (see inset in Fig. 1) is  $\sim 800 \text{ \AA}$  (*A*),  $\sim 450 \text{ \AA}$  (*B*), and  $\sim 305 \text{ \AA}$

(*C*). For each sample,  $L_b$  is sufficiently large to preclude significant quantum-mechanical interactions (evident from our calculated envelope wave functions), but allows direct electromagnetic coupling between charge oscillations in each well.

Raman scattering measurements were made under ‘‘incoming resonance’’ conditions (the incident laser photon energy was in resonance with a high-order quantum-well interband transition) to ensure that all the Raman modes were equally enhanced. Using a backscattering geometry the wave-vector transfer,  $q$ , parallel to the 2DEG layers was varied continuously by rotating the sample about an axis normal to the growth direction. Polarized spectra (incident and scattered polarizations parallel) for  $q = 1.35 \times 10^5 \text{ cm}^{-1}$  for each sample are shown in Fig. 2. In contrast to previous observations,<sup>10</sup> the OP mode is only slightly broader than the AP mode, probably because of reduced dopant scattering here. The hot photoluminescence (PL) background is associated with the interband transition responsible for the Raman

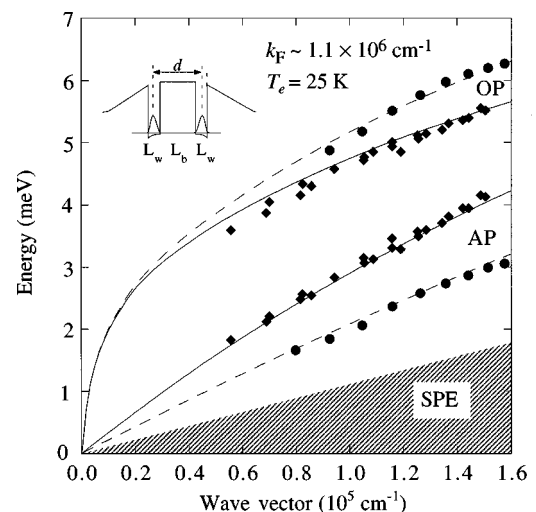


FIG. 1. Dispersion of the optic and acoustic plasmons for samples *A* ( $\blacklozenge$ ) and *C* ( $\bullet$ ). The range of possible SPEs for the experimentally determined number densities (giving  $k_F = 1.1 \times 10^6 \text{ cm}^{-1}$ ) are shown as the dashed region. The inset shows the calculated first subband envelope wave functions for sample *A*. The inter 2DEG separation,  $d$ , as well as the barrier width  $L_b$ , and the well width  $L_w$  are also shown.

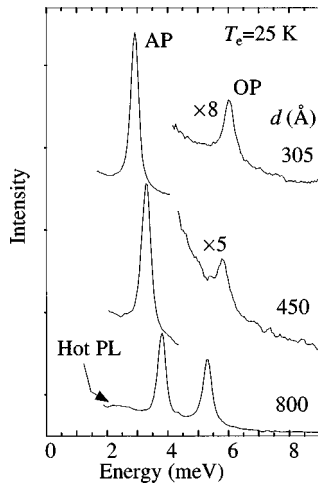


FIG. 2. Spectra from samples A ( $d \sim 800 \text{ \AA}$ ), B ( $d \sim 450 \text{ \AA}$ ), C ( $d \sim 305 \text{ \AA}$ ).  $q \sim 1.35 \times 10^5 \text{ cm}^{-1}$  and the number densities for all three samples are all approximately equal. The ‘‘hot PL’’ background is also visible. (OP, optic plasmon; AP, acoustic plasmon). The electron temperature  $T_e = 25 \text{ K}$ .

resonance. No signal was observed with the incident and scattered polarizations orthogonal. Figure 1 shows the measured dispersions for the OP and AP modes for samples A and C out to  $q \sim 1.6 \times 10^5 \text{ cm}^{-1}$  ( $\sim 0.2k_F$ , the Fermi wave vector for the sample areal 2DEG densities determined below).

Theoretical plasmon dispersions and Raman scattering spectra were obtained from the charge-density response function, calculated within the RPA, using the full layer structure and self-consistently determined wave functions for the quantum-well states.<sup>11,12</sup> It was assumed that only one sub-band in each well was occupied (i.e., intersubband transitions were ignored) and that the sub-bands dispersed parabolically. The Hubbard correction to the electron polarizability given by Jonson<sup>13</sup> (local-field factor,  $G(q) = q/[2(q^2 + k_F^2)^{1/2}]$ ) was used to account for exchange-correlation effects. The electron number densities in the two wells,  $N_1$  and  $N_2$ , were used to fit the calculations to the measured dispersions. Excellent fits were obtained with  $N_1$  and  $N_2$  both equal to  $1.97 \times 10^{11} \text{ cm}^{-2}$  (A),  $2.05 \times 10^{11} \text{ cm}^{-2}$  (B), and  $2.00 \times 10^{11} \text{ cm}^{-2}$  (C). (The individual values of  $N_1$ ,  $N_2$  were estimated to be accurate to 5%, with the total density  $N_1 + N_2$  accurate to 1%, reflecting the relative insensitivity of the fits to the values of  $N_1$  and  $N_2$  for a given total density.) These are  $\sim 70\%$  larger than those obtained from Shubnikov–de Haas measurements in the dark because of the different illumination conditions; they are, however, consistent with the Fermi energy  $E_F$  determined from the width of the quantum well PL. Thus, under illumination the number densities for the three samples were roughly equivalent; the principal difference was thus the inter-2DEG separation,  $d$ . As expected from simple theory, the energy separation between the two modes increases as  $d$  decreases (Fig. 2).

The ratio of the AP and OP Raman intensities is strongly dependent on the laser wavelength in the semiconductor and on  $d$ ;<sup>6</sup> the experimental ratios are 1.3 (A), 35 (B), and 24 (C), and the RPA calculations give 1.36 (A), 77 (B), and 3.5 (C). These discrepancies can be ascribed to difficulties

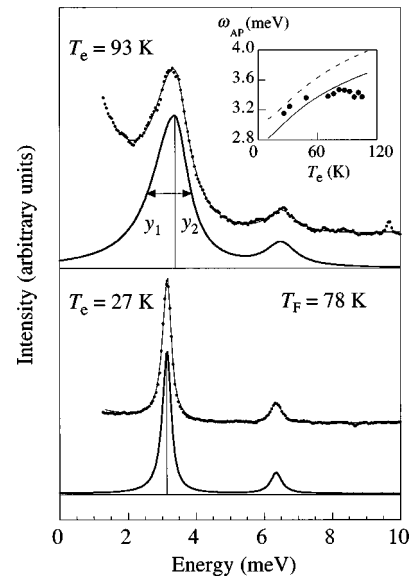


FIG. 3. Experimental spectra for  $T_e = 27 \text{ K}$  and  $T_e = 93 \text{ K}$  (dots) for sample C; fitted spectra with the hot and the band-gap PL subtracted are shown as the lower curves, displaced vertically for clarity. The Fermi temperature  $T_F$  for these samples was  $\sim 78 \text{ K}$ . The half widths at half-maximum discussed in the text,  $y_1$  and  $y_2$ , are defined as shown. The inset shows the variation of acoustic plasmon energy  $\omega_{AP}$  with  $T_e$  along with calculated energies using the RPA (straight line) and the RPA with the Hubbard correction (dashed line).

in tuning the laser energy exactly to the incoming resonance, and on  $\sim 5\%$  uncertainties in the well widths; our theory also models nonresonant Raman scattering only.<sup>14</sup> However, bearing in mind these limitations, good agreement is obtained for samples A and B.

The effect of the electron temperature  $T_e$  was studied by varying  $T_L$ , the lattice temperature, for sample C.  $T_e$  under illumination was determined from the line shape of the quantum well PL, assuming that the electron and hole temperatures were equal and that the hole density was entirely photogenerated. Illumination heated the electron gas substantially at low  $T_L$ , while  $T_e$  and  $T_L$  converged at  $\sim 100 \text{ K}$ . As  $T_L$  increased, the band gap and hence the Raman resonance energy fell and it was necessary to alter the laser frequency to maintain resonance conditions. The range over which the plasmons could be observed was limited by both the band gap and the hot PL, which overwhelm the plasmon signals at higher temperatures.

The inset in Fig. 3 shows a plot of the acoustic plasmon energy  $\omega_{AP}$  vs.  $T_e$  with  $q = 1.6 \times 10^5 \text{ cm}^{-1}$ . The two theoretical curves, one including a Hubbard correction (dashed) and one not (solid), both show an upward trend ascribable to the increased smearing of the Fermi surface as  $T_e$  rises. The failure of the theory to model the data successfully may be due to exchange-correlation effects beyond the Hubbard correction to the RPA, as has been demonstrated for intersubband plasmons.<sup>15</sup>

Spectra for  $T_e = 27 \text{ K}$  and  $T_e = 93 \text{ K}$  with  $q = 1.6 \times 10^5 \text{ cm}^{-1}$  are shown in Fig. 3. The OP broadens slightly and symmetrically as  $T_e$  rises, but the AP becomes even broader and markedly asymmetric. The OP is likely to be

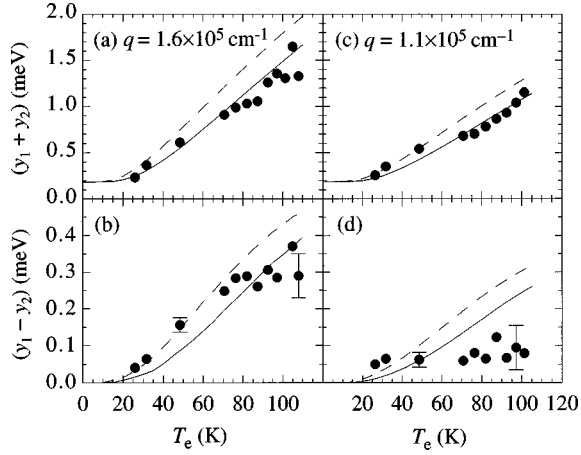


FIG. 4. The total acoustic plasmon width ( $y_1 + y_2$ ) (with Gaussian contributions removed) for (a)  $q = 1.6 \times 10^5$  and (c)  $q = 1.1 \times 10^5$   $\text{cm}^{-1}$ . Asymmetric Landau damping contribution ( $y_1 - y_2$ ), as a function of  $T_e$  for (b)  $q = 1.6 \times 10^5$  and (d)  $q = 1.1 \times 10^5$   $\text{cm}^{-1}$ . Experimental points (●) and calculations using the RPA (straight line) and the RPA with the Hubbard correction (dashed line) are shown.

more susceptible to scattering from, e.g., acoustic phonons, interface roughness, and remote ionized impurities than is the AP, for which the electric fields are localized in the inter-2DEG region, away from the dopant layers, and interact with a smaller sample volume. We therefore ascribe the asymmetry and extra broadening of the AP principally to Landau damping due to the SPE continuum which lies just below it (Fig. 1).

To quantify these effects a line-shape analysis was carried out on the AP peaks for a range of values of  $T_e$ . The experimental width includes Gaussian contributions (arising from the spectrometer resolution, the finite spread in  $q$ , inhomogeneous broadening, etc.) and contributions from single-particle relaxation and Landau damping. These combine according to

$$\Delta\omega_L\Delta\omega_{\text{tot}} + (\Delta\omega_G)^2 = (\Delta\omega_{\text{tot}})^2, \quad (1)$$

where  $\Delta\omega_L$  ( $\Delta\omega_G$ ) is the Lorentzian (Gaussian) contribution to the total half width at half maximum (HWHM)  $\Delta\omega_{\text{tot}}$ . Adapting the analysis of Dobryakov,<sup>16</sup> the total Gaussian contribution was estimated to be 0.05 meV, in good agreement with the half width of the Rayleigh scattered laser line. Because the AP line shape is asymmetric, HWHMs on either side were measured and Eq. (1) used to remove  $\Delta\omega_G$  in each case to produce  $y_1$  and  $y_2$ , the HWHMs of the Lorentzians underlying the low- and high-energy sides (see inset, Fig. 4). The lower curves in Fig. 3 show spectra fitted in this way, after subtraction of the hot and band-gap PL backgrounds.

Corresponding line shapes were calculated from the imaginary part of the density-density correlation function,<sup>12</sup> using the Lindhard expression for the free-electron polarizability evaluated at finite temperature by using the method of Flensberg and Hu,<sup>8</sup> adapted to incorporate damping due to single-particle relaxation. A Mermin correction was not included. For sample C, the single-particle relaxation time was estimated as 3.5 ps using a Dingle fit to Shubnikov–de Haas

measurements; this corresponds to a plasmon FWHM of 0.19 meV at  $T_e = 0$  K. Calculations were also carried out incorporating the  $T_e = 0$  K Hubbard correction to the electron polarizability. As with the experimental spectra, values for  $y_1$  and  $y_2$  (see above) were extracted as parameterizations of the line shapes.

Figures 4(a) and 4(c) show plots of the experimental and calculated total AP width ( $y_1 + y_2$ ) vs  $T_e$  for  $q = 1.6 \times 10^5$   $\text{cm}^{-1}$  and for  $q = 1.1 \times 10^5$   $\text{cm}^{-1}$ ; the experimental points are closer to the Hubbard corrected curve (dashed) at low  $T_e$  ( $\leq 50$  K) and to the uncorrected RPA curve (solid) for higher  $T_e$ . Nevertheless, the calculations reproduce the total AP width well, implying that the principal temperature-dependent mechanism observed is indeed Landau damping, since only this is implicitly included in the calculations. It is important to note that there are no free parameters in the calculation: the plasmon FWHM at  $T_e = 0$  K has been fixed from our determination of the single-particle relaxation time.

For a given  $T_e$  it is expected that the lower-energy side of the AP peak will be more affected by Landau damping than the higher because the SPE continuum lies below the AP dispersion curve. A direct measure of this is  $(y_1 - y_2)$ , which is plotted in Figs. 4(b) and 4(d) for both experiment and theory, again for both  $q$  values. It is expected that  $(y_1 - y_2) \rightarrow 0$  as  $T_e \rightarrow 0$  K (the peak shape would be a symmetric Lorentzian) and increase with  $T_e$ , because the lower side of the AP broadens faster as the SPE continuum broadens upwards in energy. Experimentally for  $q = 1.6 \times 10^5$   $\text{cm}^{-1}$  [Fig. 4(b)],  $(y_1 - y_2)$  increases with  $T_e$  at low  $T_e$  as expected, but at higher temperatures ( $T_e \sim 70$  K) it becomes roughly constant. For low  $q = 1.1 \times 10^5$   $\text{cm}^{-1}$  [Fig. 4(d)] the discrepancy between experiment and theory is greater and there is essentially no observable change in  $(y_1 - y_2)$  over the measured temperature range. Thus our calculations suggest a continuous increase in  $(y_1 - y_2)$  with rising  $T_e$ —contrary to experiment, where it becomes approximately constant at higher  $T_e$  for both values of  $q$ . This suggests a flattening of the SPE distribution over the width of the plasmon—i.e., the damping becomes more uniform in energy compared to our calculations at temperatures of the order of  $0.5 \sim 1.0 T_F$ , the Fermi temperature.

For both values of  $q$  for low  $T_e$  the inclusion of exchange-correlation effects, using the 0 K Hubbard correction, is necessary—and indeed sufficient—to obtain agreement between experiment and theory. Conversely, at higher  $T_e$  the calculations without the Hubbard correction match the observations better (with the exception of the asymmetry at low  $q$ ), presumably because the increasing thermal energy of the electrons reduces the significance of correlation effects and the Hubbard correction for 0 K overestimates their magnitude at higher  $T_e$ . The temperature and wave-vector dependence of the asymmetric Landau damping ( $y_1 - y_2$ ) is intriguing and unexplained.

In conclusion, by using inelastic light scattering we have observed the wave-vector dependent behavior of the plasmon modes of a double-quantum-well system to which transport measurements are insensitive. The dispersions of both optic and acoustic modes have been measured (up to  $\sim 0.2 k_F$ ) and successfully modeled within the RPA using only the number densities in the wells as fitting parameters. Qualitative agree-

ment has been obtained for the variation in the intensity ratio of the acoustic to the optic plasmon with inter-2DEG separation.

Observations of temperature effects in the Landau damping of the acoustic plasmon have also been made, and these have been modeled within the RPA with no adjustable parameters, incorporating the 0 K Hubbard correction to account for interlayer-exchange effects. Calculations of the total AP linewidth were in good agreement with experiment and illustrate clearly the decline in the importance of interlayer exchange effects as  $T_e$  rises. At low temperatures ( $T_e < T_F/2$ ) good quantitative agreement was obtained between experiment and theory for the asymmetric Landau damping contribution using the Hubbard correction. However, for  $T_e$

$> T_F/2$ , modeling the plasmon asymmetry was less successful, and the upward shift in energy of the acoustic plasmon with increasing  $T_e$  was also overestimated in the calculations. It is not envisaged that 0 K local-field corrections within the STLS framework<sup>7</sup> will substantially improve agreement with experiment, and our work points to the need for further theoretical work on local field corrections at higher temperatures. Studies of the temperature dependence of Landau damping are likely to prove valuable experimental probes of these effects.

We thank J. T. Nicholls and N. P. R. Hill for useful discussions, and the U.K. EPSRC and the Royal Society for support.

- 
- <sup>1</sup>N. H. March and M. P. Tosi, *Adv. Phys.* **44**, 299 (1995) and references therein.
- <sup>2</sup>A. Pinczuk *et al.*, *Phys. Rev. Lett.* **63**, 1633 (1989).
- <sup>3</sup>R. Decca *et al.*, *Phys. Rev. Lett.* **72**, 1506 (1994).
- <sup>4</sup>N. P. R. Hill *et al.*, *Phys. Rev. Lett.* **78**, 2204 (1997).
- <sup>5</sup>S. Das Sarma and A. Madhukar, *Phys. Rev. B* **23**, 805 (1981).
- <sup>6</sup>G. E. Santoro and G. F. Giuliani, *Phys. Rev. B* **37**, 937 (1981).
- <sup>7</sup>L. Liu, L. Swierkowski, D. Neilson, and J. Szymanski, *Phys. Rev. B* **53**, 7923 (1996).
- <sup>8</sup>K. Flensberg and B. Y.-K. Hu, *Phys. Rev. B* **52**, 14 761 (1995).
- <sup>9</sup>See, e.g., Y. Ishii and J. Rüvalds, *Phys. Rev. B* **48**, 3455 (1993); S.-M. Cui and C.-H. Tsai, *ibid.* **44**, 12 500 (1991).
- <sup>10</sup>A. S. Bhatti *et al.*, in *Proceedings of the 23rd International Conference on the Physics of Semiconductors*, edited by M. Scheffler and Zimmerman (World Scientific, Singapore, 1996), p. 1899.
- <sup>11</sup>G. Fasol *et al.*, *Phys. Rev. B* **39**, 12 695 (1989).
- <sup>12</sup>D. Richards, J. Wagner, and J. Schmitz, *Solid State Commun.* **100**, 7 (1996); **101**, 211 (1997) and references therein.
- <sup>13</sup>M. Jonson, *J. Phys. C* **9**, 3055 (1976).
- <sup>14</sup>G. Abstreiter, M. Cardona, and A. Pinczuk, in *Light Scattering in Solids IV*, edited by M. Cardona and G. Guntherodt (Springer, Heidelberg, 1984), p. 5.
- <sup>15</sup>G. Gumbs, D. Huang, and J. P. Loehr, *Phys. Rev. B* **51**, 4321 (1995).
- <sup>16</sup>S. N. Dobryakov and Y. S. Lebedev, *Sov. Phys. Dokl.* **13**, 873 (1969).